UC Merced

UC Merced Previously Published Works

Title

Generalized Kubelka-Munk approximation for multiple scattering of polarized light.

Permalink

https://escholarship.org/uc/item/5f42q06q

Journal

Journal of the Optical Society of America A, 34(2)

ISSN

1084-7529

Authors

Sandoval, Christopher
Kim, Arnold D

Publication Date

2017-02-01

DOI

10.1364/josaa.34.000153

Peer reviewed

eScholarship.org Powered by the California Digital Library
University of California

Journal of the Optical Society of America A
OPTICS, IMAGE SCIENCE, AND VISION

Generalized Kubelka–Munk approximation for multiple scattering of polarized light

CHRISTOPHER SANDOVAL AND ARNOLD D. KIM*

Applied Mathematics Unit, University of California, Merced, 5200 North Lake Road, Merced, California 95343, USA
**Corresponding author: adkim@ucmerced.edu*

Received 18 October 2016; revised 1 December 2016; accepted 3 December 2016; posted 6 December 2016 (Doc. ID 278841); published 4 January 2017

We introduce a new model for multiple scattering of polarized light by statistically isotropic and mirror-symmetric particles, which we call the generalized Kubelka–Munk (gKM) approximation. It is obtained through a linear transformation of the system of equations resulting from applying the double spherical harmonics approximation of order one to the vector radiative transfer equation (vRTE). The result is a 32 × 32 system of differential equations that is much simpler than the vRTE. We compare numerical solutions of the vRTE with the gKM approximation for the problem in which a plane wave is normally incident on a plane-parallel slab composed of a uniform absorbing and scattering medium. These comparisons show that the gKM approximation accurately captures the key features of the polarization state of multiply scattered light. In particular, the gKM approximation accurately captures the complicated polarization characteristics of light backscattered by an optically thick medium composed of a monodisperse distribution of dielectric spheres over a broad range of sphere sizes. © 2017 Optical Society of America

OCIS codes: (290.5855) Scattering, polarization; (290.4210) Multiple scattering; (030.5620) Radiative transfer.

https://doi.org/10.1364/JOSAA.34.000153

1. INTRODUCTION

Multiple scattering of polarized light is a fundamental problem with broad applications, such as optics in the ocean, the atmosphere, and biological tissues [1]. Because scattering by a single particle causes nontrivial changes to the polarization state of light, polarization-resolved measurements provide valuable insight into the optical properties of a multiple scattering medium. The key to interpreting polarization-resolved measurements is developing a quantitative understanding of fundamental mechanisms underlying the multiple scattering of polarized light.

The vector radiative transfer equation (vRTE) provides a complete mathematical description of the 4-vector containing the Stokes parameters that give the polarization state of light [2]. In the vRTE, each of the Stokes parameters satisfies an integro-differential equation. Coupling between the Stokes parameters is due to scattering through the 4 × 4 phase matrix and possibly through boundary conditions. Analytical solutions of the vRTE are only available for relatively simple problems. For more practical problems, one must use numerical methods to compute solutions [3–7]. Nonetheless, simpler models that accurately approximate the vRTE are extremely useful for polarimetry applications. Simpler models provide an opportunity to gain valuable physical insight through the determination of the key mechanisms of the problem. This insight, in turn, can be used to solve practical problems more effectively and efficiently. For example, Soloviev *et al.* [8] introduced an approximation to the vRTE, allowing for efficient tomographic reconstructions using polarized light.

Recently, the authors have derived the Kubelka–Munk (KM) or two-flux approximation for the scalar, one-dimensional radiative transfer equation [9]. A key step in that derivation was applying the double spherical harmonics method of order one (DP_1) and linearly transforming that result to obtain the so-called generalized Kubelka–Munk (gKM) equations. The gKM equations form a 4 × 4 system of differential equations. The KM equations form a 2 × 2 system, which is obtained as an asymptotic approximation of the gKM equations in the strong scattering limit. The gKM equations were shown to give better approximations than the KM equations over a broader range of optical properties. The gKM approximation has been further extended to the scalar, three-dimensional radiative transfer equation [10]. This three-dimensional extension was shown to be an effective method for approximating the spatial characteristics of transmitted and backscattered light.

Here, we apply the gKM approximation method to the vRTE. The result is a 32 × 32 system of differential equations that provides a simple model to study multiple scattering of polarized light. We use this approximation to study the

polarization characteristics of light propagation and scattering in a slab composed of a random distribution of monodisperse spheres. We validate this approximation by comparison to full numerical solutions of the vRTE. First, we study the spatial and polarization characteristics of light inside a slab with Rayleigh scattering. For this problem, we show that the gKM approximation is quantitatively accurate. Next, we study the polarization properties of light backscattered by a half-space. Characterizing the polarization state of backscattered light is a particularly challenging problem since it contains a mixture of all orders of scattering—from first-order scattering to diffusion. For this problem, we show that the gKM approximation accurately captures the polarization characteristics of backscattered light, including the phenomenon known as circular polarization memory.

The extension of gKM approximation to the vRTE provides valuable insight into the depolarization of light due to strong multiple scattering. An asymptotic analysis of the vRTE for strongly scattering media gives a full description for the multiscale behavior of this problem [11]. In particular, this theory shows that polarized light that has penetrated deep into a strongly scattering medium becomes unpolarized and isotropic. Moreover, the spatial characteristics of the intensity are modeled by the scalar diffusion approximation. In contrast, the polarization characteristics of scattered light are due entirely to scattering in the so-called boundary layer, which is a spatial region localized to superficial depths beyond the boundary. These two solutions are connected using the method of matched asymptotics. In this context, the gKM approximation provides a simple model to study the transition from shallow (boundary layer) to deep (diffusion) penetration depths, leading to depolarization.

The remainder of this paper is as follows. In Section 2, we describe the boundary value problem for the vRTE we study here. In Section 3, we apply the DP_1 approximation to the vRTE and derive the gKM approximation. In addition, we show that the gKM approximation reduces to the scalar KM equations in the limit of strong scattering. In Section 4, we show comparisons of numerical results from the gKM approximation with those from the full vRTE for the case of Rayleigh scattering. In particular, we show that the gKM approximation accurately captures the spatial and polarization characteristics of multiply scattered light. In Section 5, we study backscattering by a half-space composed of a monodisperse distribution of dielectric spheres. For this problem, we show that the gKM approximation accurately captures the complicated behavior of the polarization state as the size of the spheres varies. We give our conclusions in Section 6. Appendix A gives details about the phase matrix.

2. VECTOR RADIATIVE TRANSFER EQUATION

Let $\hat{\mathbf{s}}$ denote the direction of propagation of an electromagnetic wave. Consider the orthonormal coordinate system, $(\hat{\mathbf{e}}_l, \hat{\mathbf{e}}_r)$, perpendicular to $\hat{\mathbf{s}}$ with $\hat{\mathbf{s}} \times \hat{\mathbf{e}}_l = \hat{\mathbf{e}}_r$. We denote the complex amplitudes of the electric field in this coordinate system by E_l and E_r. For that case, the Stokes parameters are defined as

$$\begin{aligned} I &= \langle E_l E_l^* + E_r E_r^* \rangle, \\ Q &= \langle E_l E_l^* - E_r E_r^* \rangle, \\ U &= \langle E_l E_r^* + E_r E_l^* \rangle, \\ V &= \mathrm{i}\langle E_l E_r^* - E_r E_l^* \rangle, \end{aligned} \tag{1}$$

where $\langle\cdot\rangle$ denotes statistical averaging, and $\mathrm{i} = \sqrt{-1}$. These Stokes parameters give a complete description of the polarization state of light.

Let $\mathbf{I} = (I, Q, U, V)$ denote the vector of Stokes parameters. The vRTE governs $\mathbf{I}$ in a medium that absorbs, scatters, and emits light. For a scattering medium composed of statistically isotropic and mirror-symmetric particles, it is given by [2]

$$\mu \frac{\mathrm{d}\mathbf{I}}{\mathrm{d}\tau} + \mathbf{I} = \varpi_0 \int_0^{2\pi} \int_{-1}^{1} Z(\mu, \mu', \varphi - \varphi') \mathbf{I}(\mu', \varphi', \tau) \mathrm{d}\mu' \mathrm{d}\varphi', \tag{2}$$

where $\mu = \cos\theta$ is the cosine of the polar angle θ, φ is the azimuthal angle, τ is the optical depth, ϖ_0 is the single scattering albedo, and Z is the 4×4 phase matrix giving the transformation from a Stokes vector incident in the direction given by (μ', φ') to a Stokes vector scattered in the direction given by (μ, φ). We give the expansion for Z that we use throughout this paper in Appendix A.

We seek the solution of Eq. (2) in the plane-parallel slab, $0 < \tau < \tau_0$. We prescribe a plane wave incident normally on the boundary at $\tau = 0$ through the boundary condition

$$\mathbf{I}(\mu, \varphi, 0) = \frac{1}{2\pi} \mathbf{I}_0 \delta(\mu - 1) \quad \text{on} \quad 0 < \mu \le 1 \quad \text{and} \quad 0 \le \varphi \le 2\pi, \tag{3}$$

where $\mathbf{I}_0$ gives the polarization state of the incident light. Additionally, we prescribe that no light enters into the medium at $\tau = \tau_0$ through the boundary condition

$$\mathbf{I}(\mu, \varphi, \tau_0) = 0 \quad \text{on} \quad -1 \le \mu < 0 \quad \text{and} \quad 0 \le \varphi \le 2\pi. \tag{4}$$

Although we focus on this specific problem in which a plane wave is incident normally on the plane-parallel slab, the approximation method we discuss below can take into account light incident on the slab at oblique angles.

Because of the delta function appearing in boundary condition Eq. (3), we split $\mathbf{I}$ into the following sum:

$$\mathbf{I} = \mathbf{I}_r + \mathbf{I}_d, \tag{5}$$

where $\mathbf{I}_r$ is the reduced Stokes vector, and $\mathbf{I}_d$ is the diffuse Stokes vector. The reduced Stokes vector satisfies

$$\mu \frac{\mathrm{d}\mathbf{I}_r}{\mathrm{d}\tau} + \mathbf{I}_r = 0, \tag{6}$$

subject to boundary condition Eqs. (3) and (4). It is given by $\mathbf{I}_r = (2\pi)^{-1} \mathbf{I}_0 \delta(\mu - 1) e^{-\tau}$. Consequently, $\mathbf{I}_d$ satisfies

$$\begin{aligned} \mu \frac{\mathrm{d}\mathbf{I}_d}{\mathrm{d}\tau} + \mathbf{I}_d = \varpi_0 \int_0^{2\pi} \int_{-1}^{1} Z(\mu, \mu', \varphi - \varphi') \\ \times \mathbf{I}_d(\mu', \varphi', \tau) \mathrm{d}\mu' \mathrm{d}\varphi' + \varpi_0 \mathbf{J} e^{-\tau}, \end{aligned} \tag{7}$$

subject to

$$\mathbf{I}_d(\mu, \varphi, 0) = 0, \quad \text{on} \quad 0 < \mu \le 1 \quad \text{and} \quad 0 \le \varphi \le 2\pi, \tag{8}$$

and

$$\mathbf{I}_d(\mu,\varphi,\tau_0)=0, \quad \text{on} \quad -1\le\mu<0 \quad \text{and} \quad 0\le\varphi\le 2\pi, \tag{9}$$

where $\mathbf{J}$ is given by

$$\mathbf{J}=\frac{1}{2\pi}\int_0^{2\pi} Z(\mu,1,\varphi-\varphi')\mathbf{I}_0 \mathrm{d}\varphi'. \tag{10}$$

As a particular case of the slab problem described above, we consider also the half-space problem corresponding to $0<\tau<\infty$. For this problem, we solve Eq. (7) subject to boundary condition Eq. (8) and the condition that $\mathbf{I}_d\to 0$ as $\tau\to\infty$. For this half-space problem, we study the backscattered light given by $\mathbf{I}_d$ evaluated at $\tau=0$.

3. DOUBLE SPHERICAL HARMONICS METHOD AND THE GENERALIZED KUBELKA–MUNK APPROXIMATION

Boundary condition Eq. (8) prescribes $\mathbf{I}_d$ only on the hemisphere of directions pointing into the half-space corresponding to $\mu>0$, while boundary condition Eq. (9) prescribes $\mathbf{I}_d$ only over $\mu<0$. These motivate us to represent $\mathbf{I}_d$ in terms of its components over the two hemispheres corresponding to $\mu\gtrless 0$, which we denote by $\mathbf{I}^{\pm}=\mathbf{I}_d(\pm\mu,\varphi,\tau)$ for $0<\mu\le 1$, respectively. The double spherical harmonics approximation (DP_N) corresponds to approximating $\mathbf{I}^{\pm}$ as truncated expansions in an orthogonal basis defined on the hemisphere, $\{0<\mu\le 1, 0\le\varphi\le 2\pi\}$. For the DP_1 approximation, we have the following explicit approximation [10]:

$$\mathbf{I}^{\pm}(\mu,\varphi,\tau)\approx\frac{1}{2\pi}\sum_{n=1}^{4}\Phi_n(\mu,\varphi)\mathbf{I}_n^{\pm}(\tau), \tag{11}$$

where $\Phi_1=1$, $\Phi_2=\sqrt{3}(2\mu-1)$, $\Phi_3=\sqrt{3}[1-(2\mu-1)^2]^{1/2}\cos\varphi$, and $\Phi_4=\sqrt{3}[1-(2\mu-1)^2]^{1/2}\sin\varphi$. Note that in Eq. (11), the basis functions, Φ_n, for $n=1,2,3,4$, are scalar and the expansion coefficients, $\mathbf{I}_n$, are 4-vectors containing the components of the Stokes vector projected onto the corresponding basis function. The DP_1 approximation given by Eq. (11) gives an explicit dependence on the angle variables, μ and φ. It is accurate when the angular variations of the Stokes vectors $\mathbf{I}^{\pm}$ are sufficiently smooth.

We obtain a system of equations for these expansion coefficients by multiplying each of the basis functions to Eq. (7) and integrating over the hemisphere, $\{0<\mu\le 1, 0\le\varphi\le 2\pi\}$. The result of these operations is the following 32×32 system:

$$\begin{bmatrix} A & 0\\ 0 & -A\end{bmatrix}\frac{\mathrm{d}}{\mathrm{d}\tau}\begin{bmatrix}\Psi^+\\ \Psi^-\end{bmatrix}+\begin{bmatrix}\Psi^+\\ \Psi^-\end{bmatrix} = \varpi_0\begin{bmatrix}S^{(1)} & S^{(2)}\\ S^{(3)} & S^{(4)}\end{bmatrix}\begin{bmatrix}\Psi^+\\ \Psi^-\end{bmatrix}+\varpi_0\begin{bmatrix}\Gamma^+\\ \Gamma^-\end{bmatrix}e^{-\tau}. \tag{12}$$

We call Eq. (12) the polarized DP_1 system. Here, $\Psi^{\pm}=(\mathbf{I}_1^{\pm},\mathbf{I}_2^{\pm},\mathbf{I}_3^{\pm},\mathbf{I}_4^{\pm})$ is the 16-vector containing the four expansion 4-vectors in Eq. (11). Let $\mathbf{J}^{\pm}=\mathbf{J}(\pm\mu,\varphi)$ for $0<\mu\le 1$. Then, the subvectors $\Gamma_n^{\pm}$ for $n=1,2,3,4$ of $\Gamma^{\pm}=(\Gamma_1^{\pm},\Gamma_2^{\pm},\Gamma_3^{\pm},\Gamma_4^{\pm})$ in Eq. (12) are defined according to

$$\Gamma_n^{\pm}=\int_0^{2\pi}\int_0^1 \mathbf{J}^{\pm}(\mu,\varphi)\Phi_n(\mu,\varphi)\mathrm{d}\mu\mathrm{d}\varphi,\ n=1,2,3,4. \tag{13}$$

The system given in Eq. (12) is to be solved with the boundary conditions

$$\Psi^+(0)=0, \tag{14a}$$

$$\Psi^-(\tau_0)=0. \tag{14b}$$

These boundary conditions are derived by projecting boundary condition Eqs. (8) and (9) onto the basis functions, Φ_n for $n=1,2,3,4$.

The diagonal blocks of the matrix appearing on the left-hand side of Eq. (12) are given in terms of $A=M\otimes\mathbb{I}_4$, where $\otimes$ denotes the Kronecker product, $\mathbb{I}_4$ is the 4×4 identity matrix, and M is the 4×4 matrix whose entries are

$$M_{ij}=\frac{1}{2\pi}\int_0^{2\pi}\int_0^1\Phi_i(\mu,\varphi)\Phi_j(\mu,\varphi)\mu\mathrm{d}\mu\mathrm{d}\varphi \tag{15}$$

for $i,j=1,2,3,4$. These integrals and the Kronecker product can be readily computed to obtain

$$A=\frac{1}{2}\begin{bmatrix}\mathbb{I}_4 & \frac{1}{\sqrt{3}}\mathbb{I}_4 & 0 & 0\\ \frac{1}{\sqrt{3}}\mathbb{I}_4 & \mathbb{I}_4 & 0 & 0\\ 0 & 0 & \mathbb{I}_4 & 0\\ 0 & 0 & 0 & \mathbb{I}_4\end{bmatrix}. \tag{16}$$

Each of the 16×16 matrices, $S^{(1)}$, $S^{(2)}$, $S^{(3)}$, and $S^{(4)}$, appearing in the right-hand side of Eq. (12) are defined in terms of the phase matrix, Z. Let us write each of these matrices as a 4×4 block matrix:

$$S^{(k)}=\begin{bmatrix}S_{11}^{(k)} & S_{12}^{(k)} & S_{13}^{(k)} & S_{14}^{(k)}\\ S_{21}^{(k)} & S_{22}^{(k)} & S_{23}^{(k)} & S_{24}^{(k)}\\ S_{31}^{(k)} & S_{32}^{(k)} & S_{33}^{(k)} & S_{34}^{(k)}\\ S_{41}^{(k)} & S_{42}^{(k)} & S_{43}^{(k)} & S_{44}^{(k)}\end{bmatrix},\ k=1,2,3,4. \tag{17}$$

Each block, $S_{mn}^{(k)}$ for $m,n,=1,2,3,4$, is a 4×4 matrix. We denote the 16 entries of Z by $Z_{mn}(\mu,\mu',\varphi-\varphi')$ for $m,n=1,2,3,4$. We denote the (i,j)th entry of the 4×4 matrix, $S_{mn}^{(k)}$, by $[S_{mn}^{(k)}]_{ij}$. We now define the 16 entries of the $S^{(1)}$ matrix as

$$[S_{mn}^{(1)}]_{ij}=\frac{1}{2\pi}\int_0^{2\pi}\int_0^1\Phi_i(\mu,\varphi)\int_0^{2\pi}\int_0^1 Z_{mn}(\mu,\mu',\varphi-\varphi')\times\Phi_j(\mu',\varphi')\mathrm{d}\mu'\mathrm{d}\varphi'\mathrm{d}\mu\mathrm{d}\varphi, \tag{18}$$

for $i,j=1,2,3,4$ and $m,n=1,2,3,4$. The entries of $S^{(2)}$, $S^{(3)}$, and $S^{(4)}$ are given by

$$[S_{mn}^{(2)}]_{ij}=\frac{1}{2\pi}\int_0^{2\pi}\int_0^1\Phi_i(\mu,\varphi)\int_0^{2\pi}\int_0^1 Z_{mn}(\mu,-\mu',\varphi-\varphi')\times\Phi_j(\mu',\varphi')\mathrm{d}\mu'\mathrm{d}\varphi'\mathrm{d}\mu\mathrm{d}\varphi, \tag{19}$$

$$[S_{mn}^{(3)}]_{ij}=\frac{1}{2\pi}\int_0^{2\pi}\int_0^1\Phi_i(\mu,\varphi)\int_0^{2\pi}\int_0^1 Z_{mn}(-\mu,\mu',\varphi-\varphi')\times\Phi_j(\mu',\varphi')\mathrm{d}\mu'\mathrm{d}\varphi'\mathrm{d}\mu\mathrm{d}\varphi, \tag{20}$$

and

$$[S_{mn}^{(4)}]_{ij}=\frac{1}{2\pi}\int_0^{2\pi}\int_0^1\Phi_i(\mu,\varphi)\int_0^{2\pi}\int_0^1 Z_{mn}(-\mu,-\mu',\varphi-\varphi')\times\Phi_j(\mu',\varphi')\mathrm{d}\mu'\mathrm{d}\varphi'\mathrm{d}\mu\mathrm{d}\varphi, \tag{21}$$

respectively, for $i, j = 1, 2, 3, 4$ and $m, n = 1, 2, 3, 4$. We use the expansion for Z given in Appendix A and compute the integrals above using Gauss–Legendre quadrature in μ and the repeated trapezoid rule in φ.

A. Generalized Kubelka–Munk Approximation

The gKM approximation for the scalar radiative transfer equation is the transformation of DP_1 approximation to directly model the diffuse fluxes, $F^{\pm}(\tau)$, traveling in the positive and negative $\hat{z}$ directions, respectively. It was introduced as an intermediate step in the derivation of the KM approximation from the scalar radiative transfer equation [9]. The diffuse fluxes, $F^{\pm}(\tau)$, are given in terms of the intensities $I^{\pm}$ (first components in the vectors $\mathbf{I}^{\pm}$) as [12]

$$F^{\pm}(\tau) = \int_0^{2\pi}\int_0^1 I^{\pm}(\mu, \varphi, \tau)\mu \mathrm{d}\mu \mathrm{d}\varphi. \tag{22}$$

Let $I_n^{\pm}$ denote the first components of the vectors $\mathbf{I}_n^{\pm}$ for $n = 1, 2, 3, 4$, appearing in Eq. (11). Substituting the DP_1 approximation,

$$I^{\pm} \approx \frac{1}{2\pi}\sum_{n=1}^{4}\Phi_n(\mu, \varphi) I_n^{\pm}(\tau), \tag{23}$$

into Eq. (22), we find that

$$F^{\pm}(\tau) \approx \frac{1}{2} I_1^{\pm}(\tau) + \frac{1}{2\sqrt{3}} I_2^{\pm}(\tau). \tag{24}$$

Notice that this approximation of $F^{\pm}$ as a linear combination of $I_1^{\pm}$ and $I_2^{\pm}$ is the same as multiplying the first row of A, given in Eq. (16), to $\Psi^{\pm}$. It is for this reason that we introduce the linear transformation, $\mathbf{Y}^{\pm} = A\Psi^{\pm}$. Applying this change of variables in Eq. (12), we obtain the polarized gKM equations:

$$\frac{\mathrm{d}}{\mathrm{d}\tau}\mathbf{Y}^{+} = -C^{(1)}\mathbf{Y}^{+} + C^{(2)}\mathbf{Y}^{-} + \varpi_0\Gamma^{+}e^{-\tau}, \tag{25a}$$

$$-\frac{\mathrm{d}}{\mathrm{d}\tau}\mathbf{Y}^{-} = -C^{(3)}\mathbf{Y}^{+} + C^{(4)}\mathbf{Y}^{-} + \varpi_0\Gamma^{-}e^{-\tau}, \tag{25b}$$

where $C^{(1)} = (\mathbb{I}_{16} - \varpi_0 S^{(1)})A^{-1}$, $C^{(2)} = \varpi_0 S^{(2)}A^{-1}$, $C^{(3)} = \varpi_0 S^{(3)}A^{-1}$, and $C^{(4)} = (\mathbb{I}_{16} - \varpi_0 S^{(4)})A^{-1}$. Here, $\mathbb{I}_{16}$ denotes the 16×16 identity matrix. The system given in Eq. (25) is to be solved with the following boundary conditions:

$$\mathbf{Y}^{+}(0) = 0, \tag{26a}$$

$$\mathbf{Y}^{-}(\tau_0) = 0. \tag{26b}$$

We propose the system of equations given in Eq. (25) subject to boundary condition Eq. (26) as a model for multiple scattering of polarized light. Instead of solving the vRTE, this polarized gKM approximation is just a 32×32 system. Boundary conditions for this system are prescribed naturally because they are defined over the half-ranges on which boundary conditions for the vRTE are prescribed. Consequently, they do not require the introduction of additional approximations beyond the projection onto the basis functions, $\{\Phi_n\}$. The main complication in using this model is computing the matrix entries for $C^{(1)}$, $C^{(2)}$, $C^{(3)}$, and $C^{(4)}$ and the $\Gamma^{\pm}$ vectors. However, those can all be computed as a preprocessing step. In fact, this boundary value problem can be solved using the same method used for the scalar problem [9,10]. The only difference is that the size of the system is larger.

B. Strong Scattering Limit

By studying the gKM approximation for the scalar radiative transfer equation in the strong scattering limit, we have obtained the KM approximation [9]. By applying this same methodology to Eq. (25), we will presumably derive a polarized version of the KM approximation. A complete analysis of this problem is given elsewhere [13]. We summarize the results here.

Consider the homogeneous problem for Eq. (12). We seek solutions for the homogeneous problem of the form $(\Psi^{+}, \Psi^{-}) = (\mathbf{U}, \mathbf{V})e^{\lambda\tau}$ resulting in the following generalized eigenvalue problem:

$$\lambda\begin{bmatrix} A & 0 \\ 0 & -A \end{bmatrix}\begin{bmatrix}\mathbf{U}\\ \mathbf{V}\end{bmatrix} + \begin{bmatrix}\mathbf{U}\\ \mathbf{V}\end{bmatrix} = \varpi_0\begin{bmatrix} S^{(1)} & S^{(2)} \\ S^{(3)} & S^{(4)}\end{bmatrix}\begin{bmatrix}\mathbf{U}\\ \mathbf{V}\end{bmatrix}. \tag{27}$$

The eigenvalues, λ, in Eq. (27) come in $\pm$ pairs, so that for every eigenvalue λ, another eigenvalue is $-\lambda$. By studying Eq. (27) in the asymptotic limit of strong scattering corresponding to $\varpi_0 \to 1^{-}$, we find that for the smallest eigenvalues in magnitude, $\pm\lambda \to 0^{\pm}$. The eigenvectors for these vanishing eigenvalues are *completely unpolarized*. Furthermore, it can be shown by projecting Eq. (12) onto these completely unpolarized eigenvectors that we obtain the scalar KM approximation:

$$\frac{dF^{+}}{d\tau} = -(K + S)F^{+} + SF^{-}, \tag{28a}$$

$$-\frac{dF^{-}}{d\tau} = -(K + S)F^{-} + SF^{+}, \tag{28b}$$

with $S = \frac{3}{4}(1 - g) - (1 - \varpi_0)$, and $K = 2(1 - \varpi_0)$.

In fact, these results show that there is no polarized version of the KM approximation. Attempting to derive one simply leads to the scalar KM approximation. This result is consistent with the results from diffusion theory for polarized light in which the diffusion approximation applies to completely unpolarized light and is therefore just the scalar diffusion approximation [11]. Therefore, the KM approximation is inadequate for modeling multiple scattering of polarized light, except in the extreme case in which light is completely unpolarized due to strong multiple scattering.

4. RAYLEIGH SCATTERING

To test the accuracy of the gKM approximation, we first consider Rayleigh scattering, in which the sizes of the particles in the medium are much smaller than the wavelength. This case is the simplest to study the multiple scattering of polarized light. Appendix A gives the expansion coefficients for Rayleigh scattering explicitly.

We solve the boundary value problem for the vRTE comprised of Eq. (7) subject to boundary condition Eqs. (8) and (9) using the discrete ordinate method described in Ref. [14]. To compare results from the vRTE with those from the gKM approximation, we compute the following quantities:

$$F_I^{\pm}(\tau) = \int_0^{2\pi}\int_0^1 I(\pm\mu, \varphi, \tau)\mu \mathrm{d}\mu \mathrm{d}\varphi, \tag{29}$$

$$F_Q^{\pm}(\tau) = \int_0^{2\pi} \int_0^1 Q(\pm\mu, \varphi, \tau)\mu \mathrm{d}\mu \mathrm{d}\varphi, \tag{30}$$

$$F_U^{\pm}(\tau) = \int_0^{2\pi} \int_0^1 U(\pm\mu, \varphi, \tau)\mu \mathrm{d}\mu \mathrm{d}\varphi, \tag{31}$$

$$F_V^{\pm}(\tau) = \int_0^{2\pi} \int_0^1 V(\pm\mu, \varphi, \tau)\mu \mathrm{d}\mu \mathrm{d}\varphi. \tag{32}$$

We solve the gKM system given by Eq. (7) subject to boundary condition Eq. (26) using the same method described for the scalar problem [9]. From the solution $\mathbf{Y}^{\pm}(\tau)$, we extract the subvectors $\mathbf{Y}_1^{\pm}(\tau)$ and use the first, second, third, and fourth components as approximations of $F_I^{\pm}$, $F_Q^{\pm}$, $F_U^{\pm}$, and $F_V^{\pm}$, respectively.

We plot example results from these computations in Fig. 1. For these results, we have set $\tau_0 = 10$, $\varpi_0 = 0.99$, and the incident polarization state to be linear with $\mathbf{I}_0 = (1, 1, 0, 0)$. For Rayleigh scattering with linear incident polarization, $U = V = 0$ identically, so we do not plot $F_U^{\pm}$ and $F_V^{\pm}$ in Fig. 1. The first column of Fig. 1 shows plots of F_I^+ (top row) and F_Q^+ (bottom row). The second column of Fig. 1 shows plots of F_I^- (top row) and F_Q^- (bottom row). The results from the vRTE solution are plotted as solid circle symbols, and the results from the gKM approximation are plotted as solid curves.

The results shown in Fig. 1 show excellent agreement between the vRTE solution and the gKM approximation over $0 \le \tau \le 10$. The gKM approximation accurately captures the qualitative behavior of the vRTE solution. Quantitative errors are most apparent for F_Q^+, but they are relatively small. In fact, we find that the maximum errors made by the gKM approximation are less than 1% for $F_I^{\pm}$ and less than 5% for $F_Q^{\pm}$.

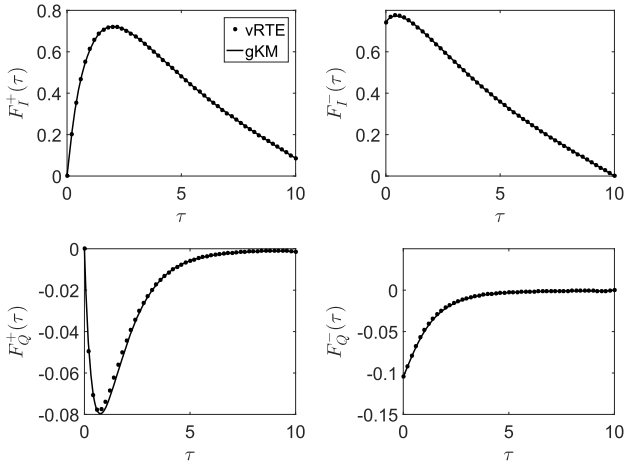

Fig. 1. Comparison of the results from the vRTE with the gKM approximation with Rayleigh scattering due to linearly polarized incident light corresponding to Stokes vector $\mathbf{I}_0 = (1, 1, 0, 0)$. The first column plots the components of $\mathbf{F}^+(\tau) = (F_I^+, F_Q^+)$, and the second column plots the components of $\mathbf{F}^- = (F_I^-, F_Q^-)$. For this problem, $F_U^{\pm} = F_V^{\pm} = 0$ identically, so we do not plot them here. Solid circle symbols correspond to the vRTE solution, and solid curves correspond to the gKM approximation.

In Fig. 2, we show results when the incident polarization state is right-handed circularly polarized with $\mathbf{I}_0 = (1, 0, 0, 1)$. All other parameters are the same as for Fig. 1. For this problem, $U = 0$ identically, so we do not plot those results in Fig. 2. In these results, we see that the gKM approximation accurately captures the behavior of V for $0 \le \tau \le 10$ in addition to I and Q. In fact, we find that the maximum errors made by the gKM approximation for this problem are less than 1% for $F_I^{\pm}$, 5% for $F_Q^{\pm}$, and 2% for $F_V^{\pm}$.

By studying the vRTE with Rayleigh scattering, we find that the gKM approximation is qualitatively and quantitatively accurate. It captures both the spatial variations and polarization changes due to multiple scattering. For example, the results shown in Figs. 1 and 2 demonstrate that light becomes depolarized as the penetration depth increases. In particular, $F_{Q,V}^{\pm} \to 0$ for $\tau > 5$ for both of these results. It is known that strong multiple scattering leads to the loss of polarization information at deep penetration depths. This depolarization is exactly what we found in studying the strong scattering limit of the gKM approximation.

Notice also that the circular polarization state of F_V^- is negative. Negative values of F_V^- indicate that the circular polarization component of backscattered light has flipped its handedness from right to left. This change in the circular polarization of backscattered light is expected since reflections of circularly polarized light change its handedness.

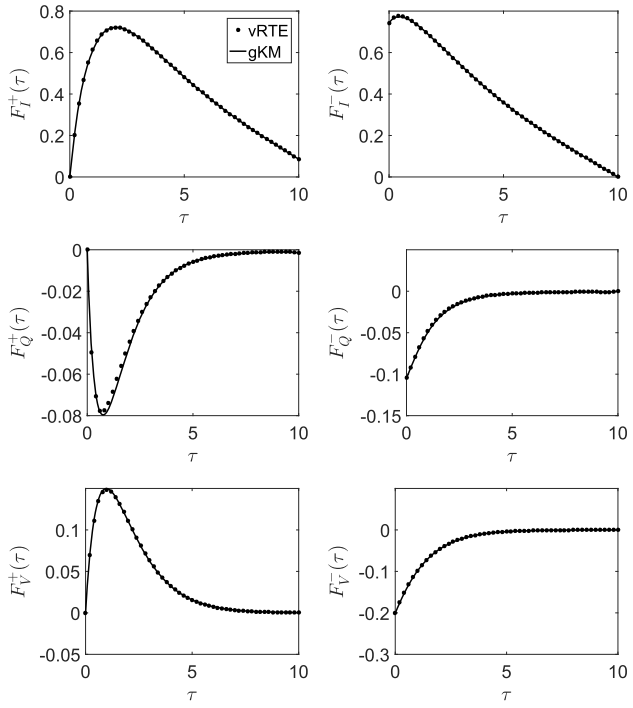

Fig. 2. Comparison of the results from the vRTE with the gKM approximation with Rayleigh scattering due to circularly polarized incident light corresponding to Stokes vector $\mathbf{I}_0 = (1, 0, 0, 1)$. The first column plots the components of $\mathbf{F}^+(\tau) = (F_I^+, F_Q^+, F_V^+)$, and the second column plots the components of $\mathbf{F}^- = (F_I^-, F_Q^-, F_V^-)$. For this problem, $F_U^{\pm} = 0$ identically, so those results are not shown here. Solid circle symbols correspond to the vRTE solution, and solid curves correspond to the gKM approximation.

5. BACKSCATTERING BY A MONODISPERSE DISTRIBUTION OF DIELECTRIC SPHERES

To evaluate the accuracy of this gKM approximation beyond Rayleigh scattering, we compare results from this approximation to numerical solutions of the vRTE using the code developed by Mishchenko *et al.* [7]. This code computes the 4×4 reflection matrix for the half-space, $0 < \tau < \infty$, by solving the vector Ambartsumian's nonlinear integral equation. The solution of this problem gives the Stokes vector exiting the half-space, $\mathbf{I}_d$ at $\tau = 0$ for $-1 \le \mu < 0$ and $0 \le \varphi \le 2\pi$. We solve this problem for a medium composed of a monodisperse distribution of dielectric spheres and evaluate that result for the case of normal incidence. To compare results from the vRTE with those from the gKM approximation, we compute

$$\mathbf{F}^{-}(0) = \int_0^{2\pi} \int_0^1 \mathbf{I}^{-}(\mu, \varphi, 0)\mu \mathrm{d}\mu \mathrm{d}\varphi, \tag{33}$$

using the same numerical quadrature rule used in that code. The components of this vector are denoted by $\mathbf{F}^{-}(0) = (F_I^{-}(0), F_Q^{-}(0), F_U^{-}(0), F_V^{-}(0))$.

In the following results, the wavelength is $\lambda = 0.55$ μm, the relative refractive index of the spheres is $m = 1.44$, and the sphere radius varies within the interval 0.01 μm $\le a \le 1$ μm. In addition, we have set $\varpi_0 = 0.99$. To compute the phase matrix, Z needed to compute Eqs. (18)–(21), we have used the expansion coefficients for Z, discussed in Appendix A, that are generated using the method described by Mishchenko *et al.* [15].

For the gKM approximation, we solve Eq. (25) subject to boundary condition Eq. (26) as we have done for the previous results for Rayleigh scattering. To compute the entries of the matrices, $C^{(1)}$, $C^{(2)}$, $C^{(3)}$, and $C^{(4)}$, we use the same expansion coefficients for Z used to compute the solution of the vRTE. Upon solution of the gKM system, we extract from $\mathbf{Y}^{-}(0)$ the subvector, $\mathbf{Y}_1^{-}(0)$, and use the first, second, third, and fourth components as approximations of $F_I^{-}(0)$, $F_Q^{-}(0)$, $F_U^{-}(0)$, and $F_V^{-}(0)$, respectively.

In Fig. 3, we show plots of $F_I^{-}(0)$ (left) and $F_Q^{-}(0)$ (right) as a function of the nondimensional Mie size parameter, $\chi = 2\pi a/\lambda$, due to Stokes vector $\mathbf{I}_0 = (1, 1, 0, 0)$ incident on the half-space. The results from the vRTE are plotted as dashed curves, and the results from the gKM approximation are plotted as solid curves. For this problem, in which linearly polarized light is incident normally on the boundary, the integrals of U and V with respect to φ over $0 \le \varphi \le 2\pi$ are zero identically [16]. It follows from Eq. (33) that $F_U^{-}(0) = F_V^{-}(0) = 0$. For this reason, we do not show results for $F_U^{-}(0)$ or $F_V^{-}(0)$ in Fig. 3.

Because ϖ_0 is fixed for this problem, the value of $F_I^{-}(0)$ computed from the vRTE is constant for all values of χ. In other words, the power backscattered by the half-space is independent of the size of the spheres in the medium. On the other hand, the value of $F_I^{-}(0)$ computed using the gKM approximation has errors since it varies with χ. Rayleigh scattering corresponds to $\chi \ll 1$ and corresponds to nearly isotropic scattering. However, for large values of χ, scattering is highly anisotropic. The gKM approximation for the scalar problem was shown to lose accuracy when the anisotropy factor

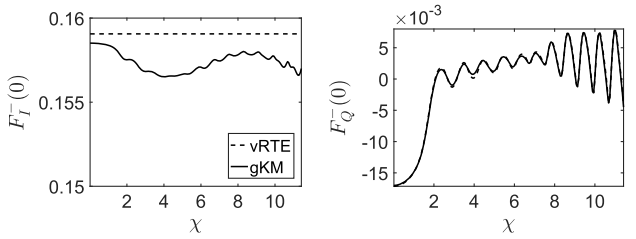

Fig. 3. Plot of $F_I^{-}(0)$ (left) and $F_Q^{-}(0)$ (right) due to Stokes vector $\mathbf{I}_0 = (1, 1, 0, 0)$ incident on the half-space as a function of the nondimensional Mie size parameter, $\chi = 2\pi a/\lambda$. The wavelength is $\lambda = 0.55$ μm, and the relative refractive index is $m = 1.44$. For this problem, $F_U^{-}(0) = F_V^{-}(0) = 0$ identically, so we do not plot them here.

grew large, especially for backscattering [9,10]. The anisotropic scattering due to the Mie spheres of varying sizes certainly contributes to the errors made by the gKM approximation shown in Fig. 3. In fact, the gKM approximation for $F_I^{-}(0)$ exhibits errors between 0.35% and 1.60% over the values of χ considered here.

Figure 3 shows that the gKM approximation accurately captures the complicated behavior of $F_Q^{-}(0)$. This qualitative agreement indicates that the gKM approximation accurately captures the polarization characteristics of backscattered light. To study the extent to which the gKM approximation does so, we consider the linear polarization ratio (LPR), defined as

$$\mathrm{LPR} = \frac{F_I^{-}(0) + F_Q^{-}(0)}{F_I^{-}(0) - F_Q^{-}(0)}. \tag{34}$$

The LPR gives the ratio of horizontal linearly polarized light to vertical linearly polarized light, so LPR $= 1$ corresponds to equal amounts of horizontally and vertically linear polarization in the polarized diffuse reflectance. From the data shown in Fig. 3, we find that the relative error made by the gKM approximation of the LPR compared to the vRTE are less than 1% for these results.

In Fig. 4, we show plots of $F_I^{-}(0)$ (top left), $F_Q^{-}(0)$ (top right), $F_U^{-}(0)$ (bottom left), and $F_V^{-}(0)$ (bottom right) as a function of χ due to Stokes vector $\mathbf{I}_0 = (1, 0, 0, 1)$ incident on the half-space, corresponding to right-handed circularly polarized light. The results from vRTE are plotted as dashed curves, and the results from the gKM approximation are plotted as solid curves. In contrast to the case in which linearly polarized light is incident normally on the half-space, we obtain nontrivial results for all four components of $\mathbf{F}^{-}(0)$ defined in Eq. (33). However, for circularly polarized light incident normally on a half-space, Stokes parameters I and Q are decoupled from Stokes parameters U and V [16]. Just as in the previous case, the gKM approximation for $F_I^{-}(0)$ computed from the vRTE solution exhibits errors between 0.35% and 1.60% over the values of χ considered here.

The bottom two plots in Fig. 4 for $F_U^{-}(0)$ and $F_V^{-}(0)$ show that gKM approximation accurately captures the polarization characteristics of backscattered light across this range of χ values. Regarding specifically circular polarization, we find that the gKM approximation accurately captures the changes in

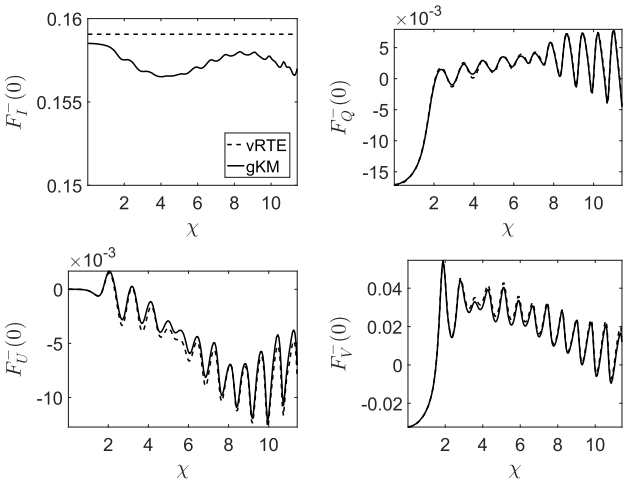

Fig. 4. Plots of $F_I^-(0)$ (top left), $F_Q^-(0)$, (top right), $F_U^-(0)$ (bottom left), and $F_V^-(0)$ (bottom right) due to Stokes vector $\mathbf{I}_0 = (1, 0, 0, 1)$ incident on the half-space as a function of the nondimensional Mie size parameter, $\chi = 2\pi a/\lambda$. The wavelength is $\lambda = 0.55$ μm, and the relative refractive index is $m = 1.44$.

sign of $F_V^-(0)$ across the range of χ values considered here. In particular, it accurately captures the change of $F_V^-(0)$ from negative (left-handed circular) to positive (right-handed circular) at $\chi \approx 1.5$.

Just as we discussed with Rayleigh scattering, it is intuitive to expect that $F_V^-(0)$ is negative since circular polarization of reflected light flips its handedness (in this case, from right to left). However, it has been observed that circularly polarized light backscattered by moderate to large spheres does not exhibit this change in handedness. For that case, backscattered light is said to exhibit circular polarization memory [17]. The change in handedness from left to right at $\chi \approx 1.5$ in the bottom plot of Fig. 4 is due to this phenomenon. Forward-peaked scattering associated with moderate to large sphere radii causes polarization memory [18]. From Fig. 4, we see that the gKM approximation accurately captures the onset of circular polarization memory as χ increases as well as the complicated behavior beyond that initial transition at $\chi \approx 1.5$.

To study the accuracy of the gKM approximation in characterizing the polarization state of backscattered light, we consider the degree of polarization (DOP) for this data, defined as

$$\mathrm{DOP} = \sqrt{[F_Q^-(0)]^2 + [F_U^-(0)]^2 + [F_V^-(0)]^2}/F_I^-(0), \quad \textbf{(35)}$$

as a function of χ. A plot of DOP computed using the vRTE results (dashed curves) and the gKM approximation (solid curves) appears in Fig. 5. For $0 < \chi \leq 3$, we find that errors made by the gKM approximation in computing the DOP are less that 5%. For $3 < \chi \leq 5.5$, errors are less than 10%. The maximum error attained is 21% for $\chi \approx 11$. The likely reason for the increase in error for larger χ is that the gKM approximation given in Eq. (11) is too simple to take into account forward-peaked scattering associated with larger values of χ. A higher-order approximation may achieve better quantitative results. Nonetheless, we find that the gKM approximation accurately captures the qualitative features of the polarization

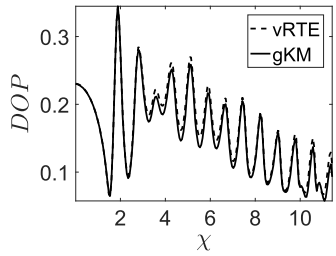

Fig. 5. Plot of the DOP defined in Eq. (35) for the data shown in Fig. 4.

characteristics of backscattered light and offers a quantitatively accurate model for small-to-moderate-sized spheres.

6. CONCLUSIONS

We have introduced the gKM approximation for the vRTE. It is a 32×32 system of differential equations derived from linear transforming the system of equations resulting from applying the double spherical harmonics method of order one to the vRTE. Consequently, it is much simpler to solve than the vRTE.

We compared results from the gKM approximation with numerical solutions of the vRTE with Rayleigh scattering. Those results show that the gKM approximation accurately captures the spatial and polarization characteristics of light propagation and scattering in a slab composed of Rayleigh scatterers. Moreover, we found that the gKM approximation provides quantitatively accurate results with maximum errors of less than 5%.

Additionally, we have used the gKM approximation to study the polarization characteristics of light backscattered by a half-space composed of a monodisperse distribution of spheres. We compared results from the gKM approximation with numerical solutions of the vRTE for a broad range of the nondimensional Mie size parameter values, $0 < \chi < 12$. For linearly polarized incident light, we found that the gKM approximation for the linear polarization ratio, LPR, is quantitatively accurate over a very broad range of sphere sizes with relative errors of less than 1%. For circularly polarized incident light, we found that the gKM approximation accurately captures the complicated features of the polarization state of backscattered light, including the transition into circular polarization memory for moderate to large spheres. However, the gKM approximation is less accurate quantitatively with respect to the DOP across the full range of χ values considered here with a maximum error of 21%. For sphere sizes within the range $0 < \chi \leq 3$, errors are less than 5%. For this reason, we conclude that the gKM approximation is most useful for this small to moderate range of sphere sizes.

From these results, we have found that the gKM approximation captures the polarization characteristics of scattered light accurately. Because this gKM approximation is the result of a systematic derivation from the vRTE, it extends readily to other problems. For example, we can extend the gKM approximation to the three-dimensional vRTE just as we have done for the scalar problem [10]. The result would be a 32×32 system

of partial differential equations. This approximation can also be extended to time-dependent problems to study the propagation and scattering of pulses in a multiple scattering medium.

Because the gKM approximation is substantially easier to solve than the vRTE, and it accurately captures the polarization characteristics of backscattered light, we believe that this approximation will be very useful for practical applications that make use of polarization-resolved measurements of scattered light.

APPENDIX A: THE PHASE MATRIX

Using the convention used by Siewert [4], the phase matrix, $\mathbf{Z}(\mu, \mu', \varphi - \varphi')$, is given by

$$\mathbf{Z}(\mu, \mu', \varphi - \varphi') = \sum_{m=0}^{L} \frac{1}{2}(2 - \delta_{0,m})[C^m(\mu, \mu') \cos\, m(\varphi - \varphi') + S^m(\mu, \mu') \sin\, m(\varphi - \varphi')], \tag{A1}$$

with

$$C^m(\mu, \mu') = A^m(\mu, \mu') + DA^m(\mu, \mu')D, \tag{A2}$$

where

$$S^m(\mu, \mu') = A^m(\mu, \mu')D - DA^m(\mu, \mu'), \tag{A3}$$

$$A^m(\mu, \mu') = \sum_{l=m}^{L} \mathbb{P}_l^m(\mu)\mathbb{B}_l\mathbb{P}_l^m(\mu'), \tag{A4}$$

and $D = \mathrm{diag}\{1, 1, -1, -1\}$. The matrices, $\mathbb{P}_l^m(\mu)$, in Eq. (A4) are defined as

$$\mathbb{P}_l^m(\mu) = \begin{bmatrix} P_l^m(\mu) & 0 & 0 & 0 \\ 0 & R_l^m(\mu) & -T_l^m(\mu) & 0 \\ 0 & -T_l^m(\mu) & R_l^m(\mu) & 0 \\ 0 & 0 & 0 & P_l^m(\mu) \end{bmatrix}, \tag{A5}$$

with

$$P_l^m(\cos\,\theta) = d_{0,m}^l(\theta), \tag{A6}$$

$$R_l^m(\cos\,\theta) = \frac{1}{2}[d_{2,m}^l(\theta) + d_{-2,m}^l(\theta)], \tag{A7}$$

$$T_l^m(\cos\,\theta) = \frac{1}{2}[d_{2,m}^l(\theta) - d_{-2,m}^l(\theta)], \tag{A8}$$

with $d_{km}^l(\theta)$ denoting the Wigner-d functions using the convention of Varshalovich *et al.* [19].

Different scattering laws in Eq. (A5) are defined through the matrices $\mathbb{B}_l$, which have the form

$$\mathbb{B}_l = \begin{bmatrix} \beta_l & \gamma_l & 0 & 0 \\ \gamma_l & \alpha_l & 0 & 0 \\ 0 & 0 & \zeta_l & -\varepsilon_l \\ 0 & 0 & \varepsilon_l & \delta_l \end{bmatrix}. \tag{A9}$$

For Rayleigh scattering, we have

$$\beta_0 = 1, \tag{A10}$$

$$\beta_2 = (1 - \rho)/(2 + \rho), \tag{A11}$$

$$\alpha_2 = 6(1 - \rho)/(2 + \rho), \tag{A12}$$

$$\gamma_2 = -\sqrt{6}(1 - \rho)/(2 + \rho), \tag{A13}$$

$$\delta_1 = 3(1 - 2\rho)/(2 + \rho), \tag{A14}$$

with ρ denoting the depolarization ratio [20]. All other terms are zero identically. For other scattering laws, we used the method described by Mishchenko *et al.* [15] to generate these expansion coefficients.

REFERENCES

1. A. Kokhanovsky, *Polarization Optics of Random Media* (Springer, 2003).
2. S. Chandrasekhar, *Radiative Transfer* (Dover, 1960).
3. J. E. Hansen and L. D. Travis, "Light scattering in planetary atmospheres," Space Sci. Rev. **16**, 527–610 (1974).
4. C. E. Siewert, "A discrete-ordinates solution for radiative-transfer models that include polarization effects," J. Quant. Spectrosc. Radiat. Transfer **64**, 227–254 (2000).
5. J. C. Ramella-Roman, S. A. Prahl, and S. L. Jacques, "Three Monte Carlo programs of polarized light transport into scattering media: part I," Opt. Express **13**, 4420–4438 (2005).
6. J. C. Ramella-Roman, S. A. Prahl, and S. L. Jacques, "Three Monte Carlo programs of polarized light transport into scattering media: part II," Opt. Express **13**, 10392–10405 (2005).
7. M. I. Mishchenko, J. M. Dlugach, J. Chowdhary, and N. T. Zakharova, "Polarized bidirectional reflectance of optically thick sparse particulate layers: an efficient numerically exact radiative-transfer solution," J. Quant. Spectrosc. Radiat. Transfer **156**, 97–108 (2015).
8. V. Y. Soloviev, G. Zacharakis, G. Spiliopoulos, R. Favicchio, T. Correia, S. R. Arridge, and J. Ripoll, "Tomographic imaging with polarized light," J. Opt. Soc. Am. A **29**, 980–988 (2012).
9. C. Sandoval and A. D. Kim, "Deriving Kubelka–Munk theory from radiative transport," J. Opt. Soc. Am. A **31**, 628–636 (2014).
10. C. Sandoval and A. D. Kim, "Extending generalized Kubelka–Munk to three-dimensional radiative transfer," Appl. Opt. **54**, 7045–7053 (2015).
11. A. D. Kim and M. Moscoso, "Diffusion of polarized light," Multiscale Model. Simul. **9**, 1624–1645 (2011).
12. A. Ishimaru, *Wave Propagation and Scattering in Random Media* (IEEE, 1997).
13. C. Sandoval, "Generalized Kubelka–Munk theory—a derivation and extension from radiative transfer," Ph.D. thesis (University of California, Merced, 2016).
14. J. Clark, P. González-Rodrguez, and A. D. Kim, "Using polarization to find a source in a turbid medium," J. Opt. Soc. Am. A **26**, 1129–1138 (2009).
15. M. I. Mishchenko, L. D. Travis, and A. A. Lacis, *Scattering, Absorption, and Emission of Light by Small Particles* (Cambridge University, 2002).
16. R. L.-T. Cheung and A. Ishimaru, "Transmission, backscattering, and depolarization of waves in randomly distributed spherical particles," Appl. Opt. **21**, 3792–3798 (1982).
17. F. C. MacKintosh, J. X. Zhu, D. J. Pine, and D. A. Weitz, "Polarization memory of multiply scattered light," Phys. Rev. B **40**, 9342–9345 (1989).
18. A. D. Kim and M. Moscoso, "Backscattering of circularly polarized pulses," Opt. Lett. **27**, 1589–1591 (2002).
19. D. A. Varshalovich, A. N. Moskalev, and V. K. Khersonskii, *Quantum Theory of Angular Momentum* (World Scientific, 1988).
20. J. W. Hovenier, C. V. M. van der Mee, and H. Domke, *Transfer of Polarized Light in Planetary Atmospheres: Basic Concepts and Practical Methods* (Springer, 2014), Vol. **318**.

169.236.1.253 {ts '2017-04-11 12:38:39'}